Micro-scale roughness effects on the friction coefficient of granite surfaces under varying levels of normal stress

O. Biran , Y.H. Hatzor & A. Ziv
Ben-Gurion university of the Negev, Beer-Sheva, Israel

ABSTRACT: In this paper we explore roughness and normal stress effects on the steady-state friction coefficient of granite. Our tests were performed on a single direct shear, servo controlled, apparatus. To check the validity of the direct shear apparatus, we begin with a series of classic rate and state experiments. After establishing a good agreement with published results, we proceed with measurements of micro-scale roughness effects on friction using four levels of micro roughness on polished and ground surfaces, under normal stresses between 2.5 MPa and 15 MPa. For rough sliding surfaces we observe a second order normal stress effect on friction, where under normal stresses up to 5 MPa the friction coefficient decreases with increasing normal stress; above that normal stress level and up to 12 MPa the friction coefficient increases with normal stress, beyond which the friction coefficient exhibits a constant value similar to what is observed in standard direct shear tests. We find that behavior to be roughness dependent. It diminishes with decreasing roughness, and is not at all observed if the sliding surface is extremely smooth.

1 INTRODUCTION

The slip of solid materials along a pre-existing surface is resisted by friction. The first documented study on friction was performed by Leonardo da Vinci. His finding was confirmed later by Amontons (1699), who found that the frictional force is independent of the geometrical contact area, and is equal to the ratio between the shear and normal stresses. Bowden & Tabor (1954) suggested an explanation for the independence of the friction coefficient on the geometrical contact area. In their work on metals, they noted that the surfaces are in contact only at discrete locations, or "asperities", and therefore the "real" contact area is much smaller than the geometrical area. While Amonton's law provides a good description for friction for many applications, it is not suitable for the description of unstable friction phenomena such as earthquakes (Scholz 2002). In order to model and better describe dynamic friction phenomena, rate and state friction laws were developed by Dieterich (1979) based on experimental observations. Dietrich's laws describe the friction coefficient as a function of the slip rate and a state variable (Dieterich 1979, Ruina 1983). Rate and state friction laws provide powerful tools for investigating the mechanics of earthquakes and faulting, and the incorporation of the state variable provides a means to account for complex friction memory effects and history dependence. In the past few years, concentrated efforts were invested in the improvement of rate and state friction laws by adding more variables that influence the friction coefficient, such as normal stress variations (Linker & Dieterich 1992, Richardson & Marone 1999, Boettcher & Marone 2004, Hong & Marone 2005). In this paper we present preliminary experimental results that show how roughness and normal stress effects on the steady-state friction coefficient

2 BACKGROUND

Rate and state friction was originally proposed by Dieterich (1979) on an empirical basis using an extensive body of shear tests. Experimental results show that the friction coefficient, μ, is a function of slip rate, V, and a state variable, θ, as follows (Dieterich 1979, Ruina 1983):

$$\mu = \mu^* + A\ln\left(\frac{V}{V^*}+1\right) + B\ln\left(\frac{\theta V^*}{D_c}+1\right), \quad (1)$$

where A and B are dimensionless empirical fitting parameters, D_c is a characteristic sliding distance from one steady state to another, V^* is the reference velocity, and μ^* is the coefficient of friction when the contact surface slips under a constant slip rate V^*. Various evolution laws have been proposed for the state variable. The two most commonly used state evolution laws are the 'Dieterich law' (Dieterich 1979):

$$\frac{d\theta}{dt} = 1 - \frac{V\theta}{D_c}, \tag{2}$$

and the 'Ruina law' (Ruina 1983):

$$\frac{d\theta}{dt} = -\frac{V\theta}{D_c}\ln\left(\frac{V\theta}{D_c}\right). \tag{3}$$

These laws were originally formulated for conditions of constant normal stress and were later extended by Linker & Dieterich (1992) to account for variable normal stress. In equation 2, state, and thus friction, evolve even for V = 0. At hold time, dθ/dt=1, therefore the state variable during the hold time is:

$$\theta = \theta_0 + \Delta t, \tag{4}$$

Substituting (4) in (1) shows that coefficient of friction increases with the logarithm of the hold time, i.e.:

$$\mu \propto B\ln(t). \tag{5}$$

In Ruina's evolution law any change in friction, including strengthening during quasi-stationary contact, requires slip. In either case, the condition for steady state coefficient of friction is $V\theta/D_c = 1$ and for both laws, the steady state velocity dependence is:

$$\mu_{ss} = \mu^* + (A - B)\ln\left(\frac{V_{ss}}{V^*} + 1\right). \tag{6}$$

Thus, steady state friction exhibits velocity weakening if B is greater than A, and velocity strengthening otherwise. The rate and state friction laws have been successfully used to address various geophysical problems, including simulation of crustal deformation along faults (Rice 1993, Ziv & Cochard 2006), and earthquake modeling (Marone et al. 1995, Tullis 1996, Scholz 1998).

3 EXPERIMENTAL METHODS

3.1 *Testing Apparatus*

Our tests were performed on a single direct shear, hydraulic, servo controlled apparatus (Figure 1A, 1B). Normal and shear load cell capacities are 1000 kN and 300 kN, respectively. Shear box size is 180 mm x 180 mm x 140 mm. The sample is cemented into the shear box using Portland 350 cement. Shear and dilatational displacements are monitored by 6 LVDT type displacement transducers, with a maximum range of 50 mm and 0.25% linearity full scale. Additional 4 LVDT transducers, used to monitor vertical (dilatational) displacements were mounted on four corners of the shear box; 2 LVDT transducers, used to monitor horizontal (shear) displacement were mounted on two opposite sides of the tested interface (Figure 1C). In order to obtain optimal feedback signals and control, all six transducers were mounted as closely as possible to the sliding interface. Using a computer control interface, output signals from all channels can be used as servo control variables, currently at an acquisition rate of 50 Hz. We used the average of the two shear displacement transducers output to control the sliding velocity, and used the output from the normal piston load cell to control the normal stress during sliding.

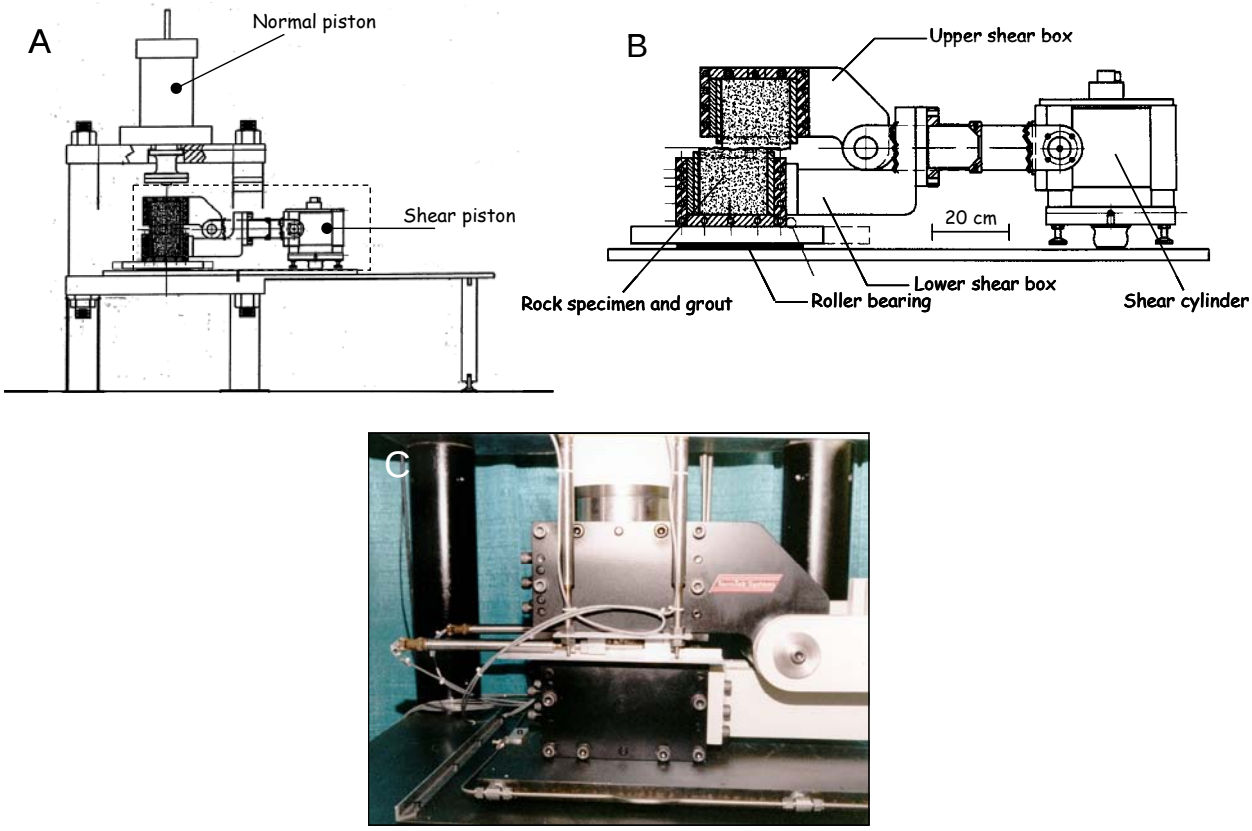

Figure 1. The direct shear system assembly. A. The complete load frame assembly. B. Close view of the shear box, shear piston and shear load frame. C. Close view on the horizontal (shear) and vertical (dilatational) displacement transducers (LVDT).

3.2 *Tested Material*

Direct shear tests were performed on machined Timna granite blocks, typically with a 10 cm by 10 cm nominal (i.e. geometric) contact area. In order to ensure that the nominal contact area remains constant during sliding, the upper block was machined to slightly smaller dimensions than the lower block.

Four surface roughness levels were examined. These were obtained with three different preparation methods: 1. Rough (SC) - roughness that results from sawing the sample with standard rock saw, 2. Smooth (SG) – roughness obtained with a standard surface grinder; 3. Surface polished by hand-lapping using a 180 Silicone Carbide powder (#180), 4. Surface polished by hand-lapping using a 220 Silicone Carbide powder (#220).

Surface roughness was measured using an optical profilometer, Zygo NewView 5000 white-light interferometer. The optical output is processed, statistically analyzed and graphically displayed using a post processing software package (MetroPro) (Figure 2B, 2C, 2D). Three statistical parameters of surface topography are used for characterising the different finished surfaces: 1. RMS – the root mean square, 2. R_a - the average distance of all points from an arbitrary plane, and 3. PV - the maximum peak to valley height over the sample area. To assess roughness anisotropy, measurements were taken parallel and perpendicular to slip direction.

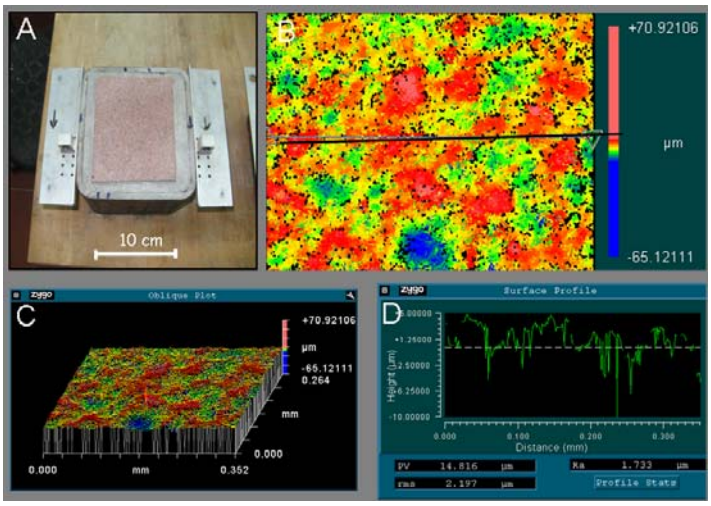

Figure 2. An example of roughness graphic display. A. Interface smoothed using surface grinder. B. Roughness distribution in plane view. C. Three dimensional view of panel B. D. Profile along the cross section in panel B.

Statistical analyses of the obtained roughness profiles indicate that there are significant differences between the studied surfaces. While the polished surfaces are nearly isotropic, the saw-cut surfaces are clearly not (Figure 3). Direct shear tests were always performed while keeping the shear direction parallel to the direction of maximum roughness.

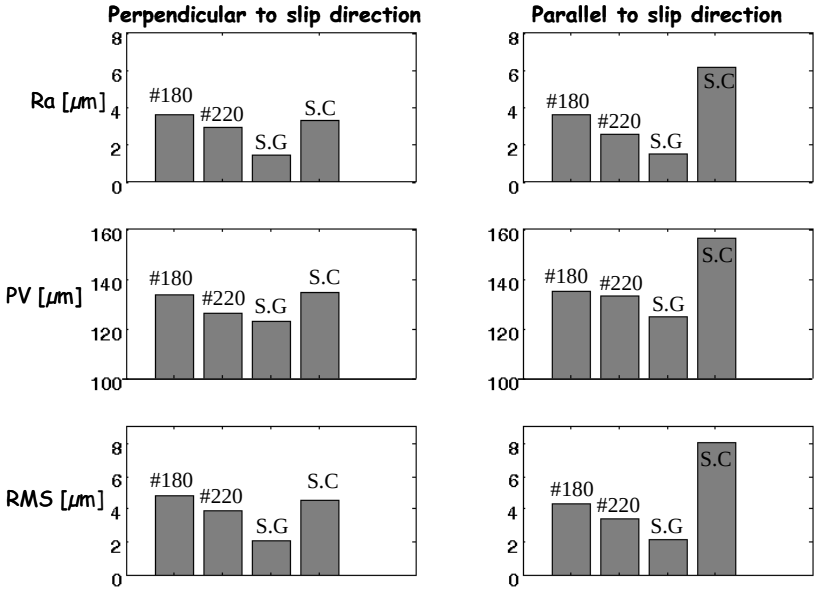

Figure 3. Statistics of roughness parameters measured using the Zygo NewView 5000 interferometer prior to the direct shear tests. Note roughness anisotropy in the saw cut samples.

3.3 *Preliminary Smoothing Segment*

In order to suppress stick-slip episodes, and to reach the displacement magnitude required for sliding at steady state, all experiments were first began with a smoothing cycle, consisting of a forward shearing segment at a constant sliding rate of 10 µm/S to a distance of 5 mm under a constant normal stress of 5 MPa followed by a backward shearing segment, under a constant normal stress of 0.2 MPa at a sliding velocity of 100 µm/S (Figure 4).

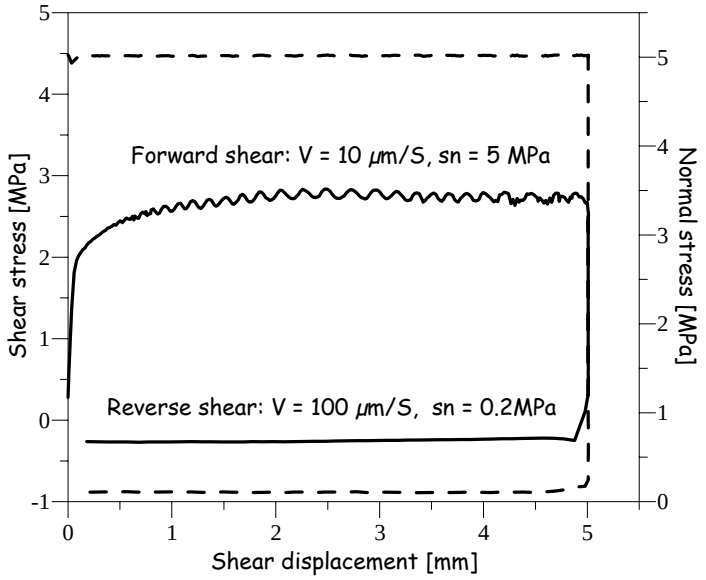

Figure 4. Preliminary smoothing segment performed prior to each experiment. Shear stress (solid line, left vertical axis) and normal stress (dashed line, right vertical axis) as a function of shear displacement.

4 REPRODUCING THE CLASSICAL RATE AND STATE EXPERIMENTS USING A DIRECT SHEAR APPPRATUS

Previous experiments that examined the effects of slip rate and contact age were performed using a double shear apparatus (Dieterich 1979, Linker & Dieterich 1992, Dieterich 1972, Kilgore et al. 1993). In the double shear configuration the net torque in the system may be negligible, whereas in the direct shear system it is not. We first reproduce some typical rate and state experiments to verify that the differences between the two testing configurations do not influence the results. Below we present three types of rate and state experiments: slide-hold-slide, velocity stepping and normal stress stepping, which were successfully reproduced with the direct shear apparatus.

4.1 *Slide – Hold – Slide experiments*

In order to examine the effect of the hold duration on the static friction coefficient Slide-Hold-Slide (SHS) experiments were preformed, similar to the procedure described by Dieterich (1972) and Dieterich & Kilgore (1994). During these experiments the normal stress was held constant at 5 MPa. Constant slip rates of 100 and 50 μm/S were imposed on the sample until a steady state friction coefficient was attained. Once steady state sliding was attained, the shear piston displacement was stopped for specified time intervals, after which shear sliding commenced at the original slip rate before the hold segment. SHS segments were repeated several times, with increasing hold interval each time. A typical result for a SHS experiment is displayed in Figure 5A for a #180 SiC surface. Inspection of Figure 5B reveals that the peak (or static) friction coefficient and consequently $\Delta\mu$ (where $\Delta\mu$ is the difference between static and initial friction coefficients), increase with hold time and slip rate, consistent with previous findings (Dieterich 1972, Dieterich & Kilgore 1994, Marone 1998). This data together with equation 5 were used to obtain the rate-and-state *B* parameter (see Table 1).

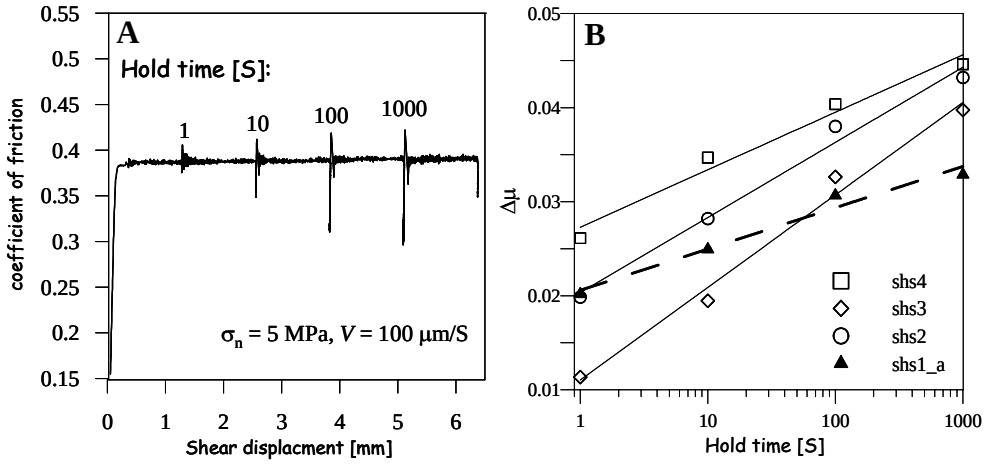

Figure 5. Result of SHS tests. A. A typical result for a single run. B. Peak less residual friction coefficient as a function of hold time (See Table 1 for regression coefficients). Solid lines V = 100 mm/S and dashed line V = 50 mm/S.

Table 1. Summary of velocity stepping and slide hold slide tests

Experiment	Normal stress [MPa]	Sliding rate [μm/S]	*B*	*A-B*	*A*	R^2
shs1_a	5	50	0.002	-	-	0.973
shs2	5	100	0.004	-	-	0.988
shs3	5	100	0.004	-	-	0.986
shs4	5	100	0.003	-	-	0.975
vs6_g1	7.5	0.0125-1.6	-	-0.006	0.006	0.984
vs4_g1	7.5	0.2-10	-	-0.006	0.005	0.991
vs3_g1	5	0.1-100	-	-0.01	0.005	0.959
vs4b_g1	2.5	0.1-100	-	-0.008	0.005	0.865
vs5b_g1	5	0.1-100	-	-0.009	0.008	0.839

shs- slide hold slide experiment, vs- velocity stepping experiment.

4.2 *Velocity stepping experiments*

We performed velocity stepping experiments, similar to those performed in the past by other researchers (Dieterich 1979, Kilgore et al. 1993, Tullis & Weeks 1986). These experiments were preformed on rough surfaces (saw cat) at slip rates between 0.0125 and 100 μm/S, and under a constant normal stress of 5 MPa for slip rats between 1 and 100 μm/S) and under 7.5 MPa for slip rates between 0.0125 and 10 μm/S. The imposed sliding velocity was increased by a factor of 10 between adjacent segments during sliding velocities between 1 and 100 μm/S and by a factor of 2 during sliding velocities between 1 and 0.0125 μm/S. We found that in response to step decrease in slip rate the coefficient of friction rapidly decreased and than rose to a new higher steady value as sliding commenced, in agreement with the previous works cited above (see Figure 6A). Furthermore, we found that the rise to a new steady state friction coefficient value roughly followed an exponential curve with a characteristic displacement magnitude D_c ranging from 1 to 1.5 μm in those tests for which D_c was estimated. The A parameter was retrieved directly from the experimental output and the value of $A - B$ was estimated by using Equation 4 (see Figure 6B); the quantitative estimates of A, B, and A-B for all the tests are listed in Table 1.

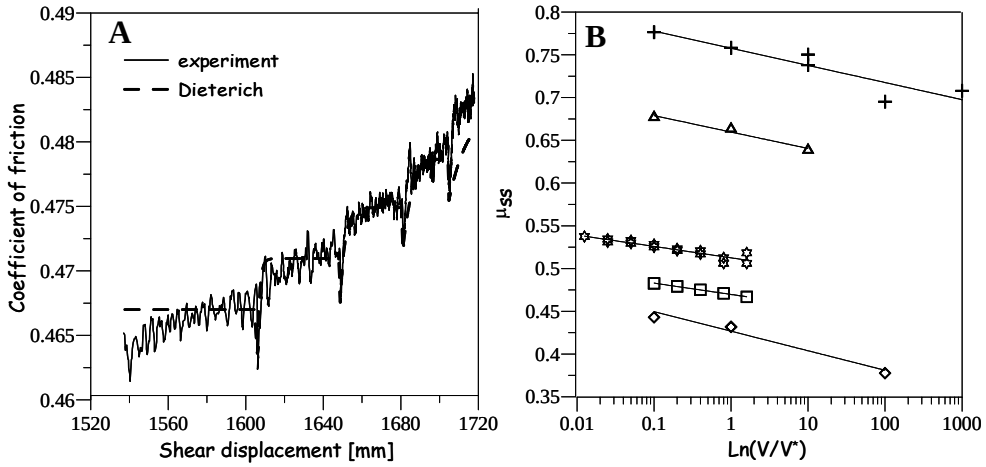

Figure 6. Result of velocity stepping experiments. A. Friction coefficient vs. shear displacement, dashed line based on Dieterich constitutive law with: A = 0.0049, $A - B$ = -0.0057 and Dc = 0.001 mm. B. Friction coefficient at steady state as a function of shear rate. See Table 1 for the slopes of the regression lines (A – B).

4.3 *Rapid normal stress stepping*

Normal stress stepping tests were performed on a rough saw-cut surface, in a manner similar to experiments reported by previous researchers (Linker & Dieterich 1992, Hong & Marone 2005). Rapid normal stress changes were imposed on the sample during steady-state sliding at a sliding velocity of 10 μm/S. The test was performed under an initial constant normal stress value of 5 MPa, and when the sample attained steady – state the normal stress level was changed by ±20% from the nominal value, at a very fast rate. The frictional response of the tested interface to changing normal stress is shown in Figure 7. In agreement with previously published results (Linker & Dieterich 1992, Hong & Marone 2005), we find that the change in normal stress was simultaneously accompanied by a linear change in shear stress, followed by a delayed non linear response, most likely due to plastic yield at contact points along the tested interface.

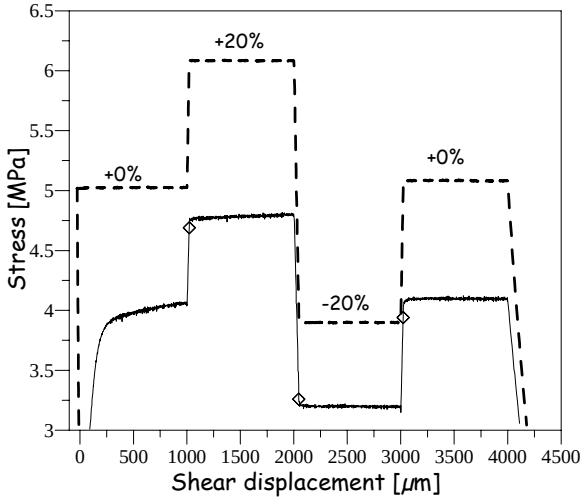

Figure 7. Normal (dashed) and shear (solid) stresses as a function of shear displacement during normal stress stepping. The diamonds indicate the end of instantaneous response

5 STEADY-STATE FRICTION DEPENNEDECE ON SURFACE ROUGHNESS

Does steady state friction depend on surface roughness? To address this question the results of direct shear tests preformed on SC (rough) and SG (smooth) surfaces are compared. These testes were carried out at various sliding velocities and normal stress. For each normal stress level the corresponding shear stress at steady state was determined graphically (Figure 8) and the results were plotted on a τ- σ space (Figure 9).

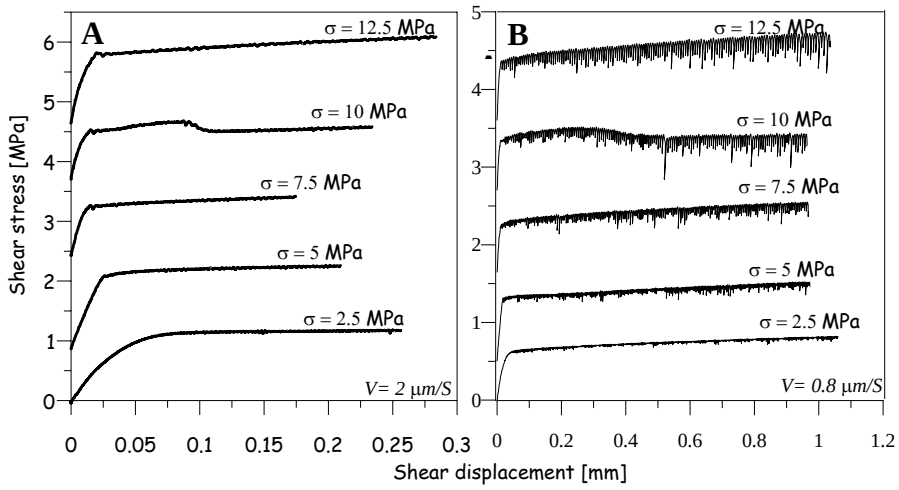

Figure 8. Shear stress vs. shear displacement under an imposed constant normal stress condition. A. V = 2 μm/S. B. V = 0.8 μm/S.

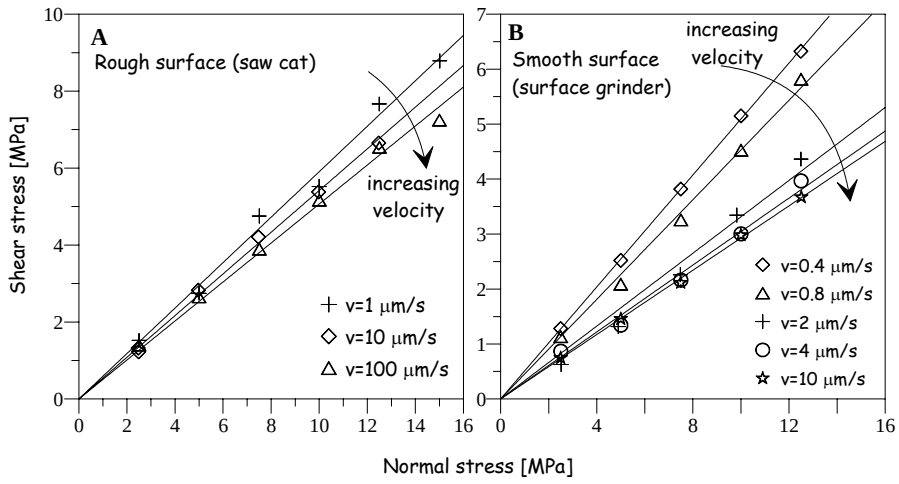

Figure 9. Obtained Coulomb criteria for different slip rates. A. Rough surfaces (saw cut). B. Smooth surfaces (surface grinder). Linear regression coefficients for each sliding velocity are listed in Table 2.

The friction coefficient for each surface and sliding velocity are listed in Table 2, along with the obtained values of the linear regression coefficient R^2. The experimental results show that the steady-state friction for either surface is velocity weakening, and that it is more velocity weakening for smooth surface then it is for rough surface (Figure 10).

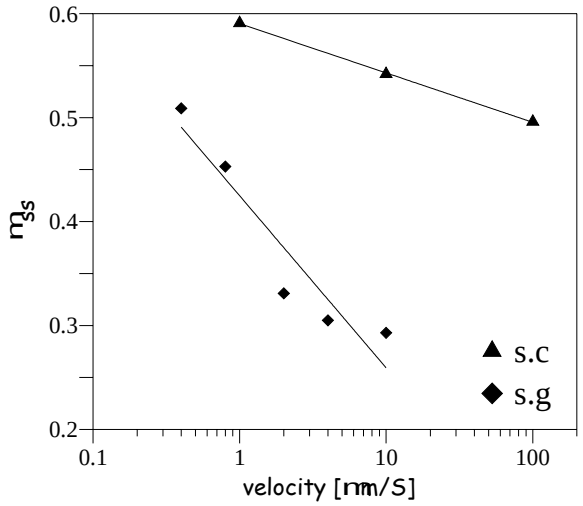

Figure 10. Friction coefficient at steady state as a function of shear rate.

Table 2. The friction coefficient that is obtained from Coulomb failure criteria

Sliding rate [μm/S]	Roughness	Friction coefficient	R^2
1	SC	0.591	0.998
10	SC	0.542	0.999
100	SC	0.495	0.999
0.4	SG	0.509	0.999
0.8	SG	0.453	0.999
2	SG	0.331	0.994
4	SG	0.305	0.997
10	SG	0.293	0.999

SC – saw cat, SG- surface grinder

6 SECOND ORDER NORMAL STRESS EFFECTS ON STEADY-STATE FRICTION

Through measurements of shear stress response to changing the normal stress during sliding under constant rate we have identified a second order effect of normal stress on the steady state friction coefficient. First steady-state sliding was obtained under a constant sliding velocity of 1 μm/S and an imposed constant normal stress. Next the normal stress was increased or decreased to a specified new target using normal stress output as the servo control parameter. Seeking the new normal stress target was performed while shear sliding continued under a displacement control mode imposed on the shear piston. Two sets of tests were thus performed. While in one, the starting normal stress was set to 15 MPa and has been decreased by 10% each time down to 2.5 MPa, in the other the starting normal stress was set to 2.5 MPa and has been increased by 10% each time up to 15 MPa. Stepping the normal stress was done at a rate of 0.05 MPa/S. Finally four types of surface finish were studied: 1) Saw Cat (SC.), 2) #180 grit of SiC, 3) #220 grit of SiC and 4) Surface grinder (SG), whose roughness statistics were reported in section 3.2. Typical result for shear stress response to descending and ascending normal stress are shown in Figures 11A and 11B respectively for saw cat surfaces.

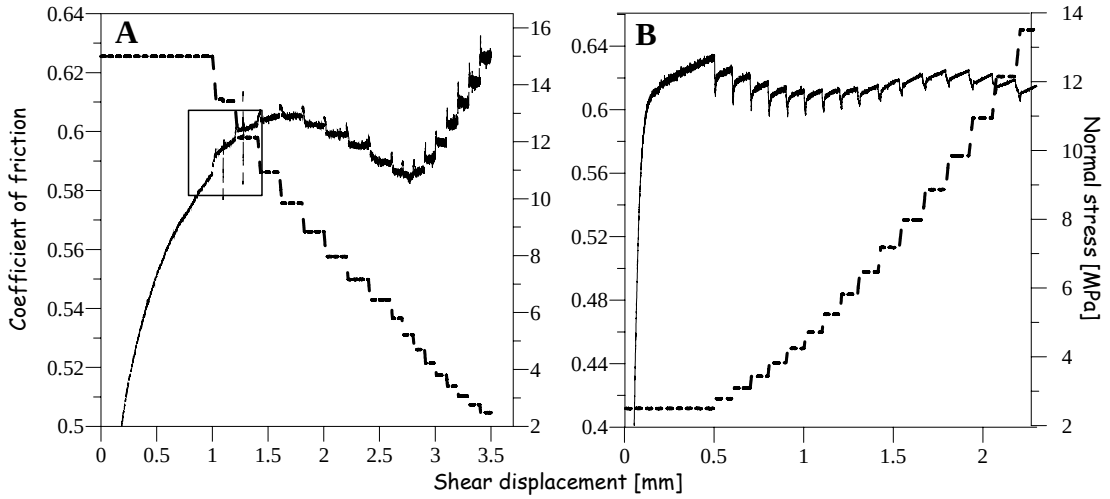

Figure 11. Friction coefficient (solid curves and left vertical axes) and normal stresses (dashed curves and right vertical axes) as a function of shear displacement for decreasing (A) and increasing (B) normal stress level during sliding at a constant rate. The box indicates a segment that did not reach steady state.

For reasons that are not presently clear to us, friction coefficients for the stress-ascending experiment (Figure 11B) failed to reach steady-state. Since here we are interested in roughness and normal stress effects on steady-state friction, the result of stress-ascending experiments will not be considered further (Figure 11B). Note the normal stress dependence of the steady-state friction coefficient of rough samples (SC). Specifically, we find that the steady-state friction coefficient decreases with increasing normal stresses for normal stresses between 2.5 and 5.22 MPa, but increases for normal stresses between 5.22 and 12.5 MPa (Figure 12A). We are unable to draw conclusions for normal stresses greater than 12.5 MPa, since for these stress levels the system did not reach steady-state (box in Figure 11A). Interestingly, the result for smooth surfaces differs radically from that for rough surfaces. Steady-state friction for smooth surfaces, increases with increasing normal stresses (Figure 12B). The differences in the friction coefficient that were obtained for each normal stress level are clear and significant (Figure 13A-C).

We rationalize our results as follows: Beginning with the rough surfaces, under the lowest tested normal stress (2.5 MPa) it seems that the influence of roughness is most pronounced with a maximum value of coefficient of friction of 0.625 at that stress level. With increasing normal stress levels the obtained coefficient of friction for steady state decreases until a minimum value of 0.583 is obtained. This value represents the lowest friction coefficient obtainable for Saw Cut surfaces under the studied normal stresses and sliding velocities. We believe that this minimum value marks the end of the role initial asperities play in the frictional response of the tested SC surfaces. When the normal stress is further increased the effect of plastic flow and healing at contact areas becomes more pronounced and therefore shear strengthening is obtained. With the smooth surfaces, however the behaviour is different. It seems that in all smooth surfaces the first shear softening stage is missing and we only get shear hardening as normal stress is increased, indicating that the role of plastic flow and healing around contact points is the dominant mechanism in initially smooth surfaces. The only difference between the samples polished by hand lapping in SiC powder (#180, #220) and the surfaces polished with mechanical surface grinder (SG) is the minimum value of the friction coefficient obtained: whilst in the surfaces polished with SiC powder the minimum value is 0.53 the surface polished with surface grinder exhibits a friction coefficient of 0.2. Note that the sample that was prepared with #180 SiC powder (Figure 12B - open triangles) exhibits shear hardening as normal stress is increased by as much as 20% with respect to the initial shear stress, representing an increase in coefficient of friction from 0.55 for low normal stresses to 0.7 for high normal stresses. This significant amount of

shear hardening can not be considered a second order effect, and is in fact in contradiction with Coulomb law. This interesting preliminary observation requires further research.

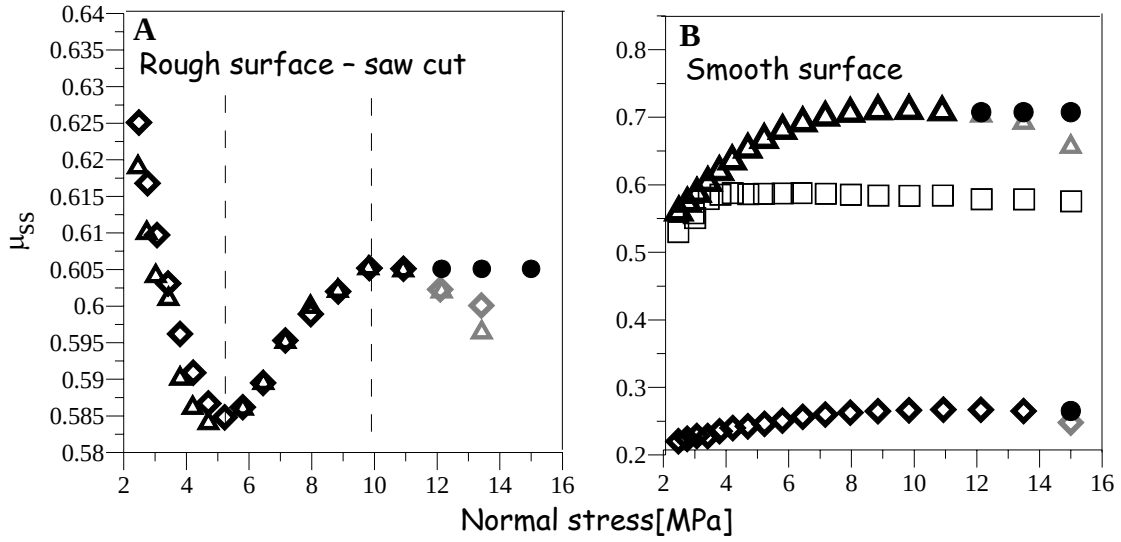

Figure 12. Steady–state friction as a function of normal stress level. (A) obtained for the two rough surfaces (saw-cut). Both tests were performed under the same conditions and similar results are obtained. Strengthening effect of asperities decreases with increasing normal stress levels up to 5.2 MPa, beyond which increase in strength is detected with increasing normal stress up to a level of 12 MPa, at which stage a constant level of friction coefficient is attained. Note that the last two segments (σn = 12.5 MPa, 15 MPa) did not reach steady state during the test (see boxes in Figure 11), the inferred friction coefficient values for these two tests are plotted in solid symbols. (B) obtained from three different surfaces: surface grinder (SG - open diamonds), polished with # 220 grit (open squares), polished with # 180 grit (open triangles). An extremely low friction coefficient of μ = 0.2 is obtained with the SG samples. A pronounced increase in friction coefficient is obtained with the polished surfaces to μ = 0.5 – 0.6. In all cases the strengthening is observed with increasing normal stress. Inferred μ values for segments where steady state was not reached during the test are plotted as solid symbols.

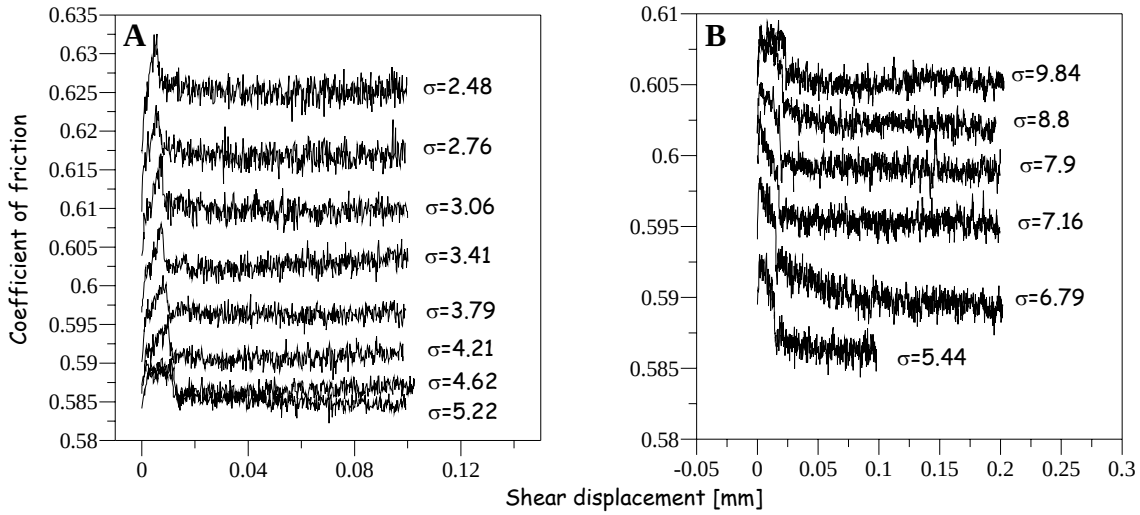

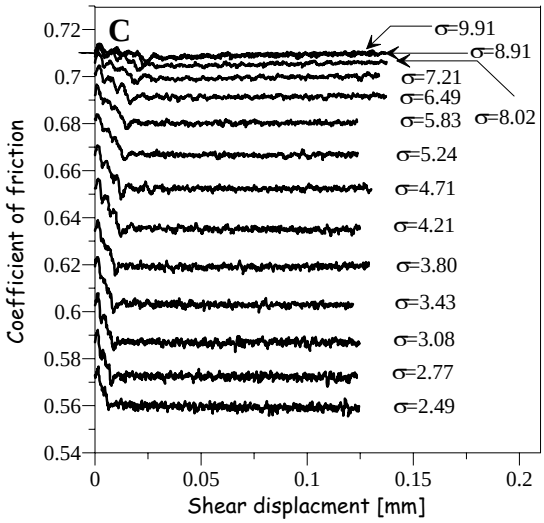

Figure 13. Obtained friction coefficients at steady state for each individual segment. A+B. Test on rough surface that presented in figure 11A. C. Test on smooth surface (#180) that presented in figure 11B.

7 SUMMARY

Using direct shear apparatus, we have reproduced some of the rate and state friction experiments including the slide-hold-slide, velocity stepping and normal stress stepping. We find that the differences between the direct and the double shear testing configurations do not influence the results. Roughness effects on steady state friction coefficient were examined by comparing constant slip rate and normal stress shear tests on surfaces of different roughness levels. We have showed, using Coulomb criterion, that the steady-state friction for all roughness levels is velocity weakening, and that it is more velocity weakening for smooth surfaces than it is for rough surfaces. Finally, through measurements of shear stress response to changing the normal stress during sliding under constant rate we have identified a second order effect of normal stress on the steady state friction coefficient. On rough surfaces, the steady state friction coefficient decreases with increasing normal stress at low normal stress (2.5-5MPa), but increases at normal stress that are higher than 5 MPa. On smooth surfaces on the other hand, steady-state friction increases with increasing normal stresses.

REFERENCES

Boettcher, M.S. & Marone, C. 2004, "Effects of normal stress variation on the strength and stability of creeping faults", *Journal of Geophysical Research*, vol. 109, B03406, doi:10.1029/2003JB002824.

Bowden, F.P. & Tabor, D. 1964, *The friction and lubrication of solids*, Oxford University Press.

Dieterich, J.H. 1972, "Time dependent friction in rocks", *Journal of Geophysical Research*, vol. 77, p. 3690-3697.

Dieterich, J.H. 1979, "Modeling of rock friction 1. Experimental results and constitutive equations", *Journal of Geophysical Research*, vol. 84, p. 2161-2168

Dieterich, J.H. & Kilgore, B.D. 1994, "Direct observation of frictional contacts: New insights for state-dependent properties", *Pure and Applied Geophysics*, vol. 143, p. 283-302.

Hong, T.C. & Marone, C. 2005, "Effects of normal stress perturbations on the frictional properties of simulated faults", *Geochemistry Geophysics Geosystems*, vol. 6, Q03012, doi:10.1029/2004GC00082.

Kilgore, B.D., Blanpied, M.L. & Dieterich, J.H. 1993, "Velocity dependent friction of granite over a wide range of conditions", *Geophysical Research Letters*, vol. 20, p. 903-906.

Linker, M.F. & Dieterich, J.H. 1992, "Effects of Variable Normal Stress on Rock Friction - Observations and Constitutive-Equations", *Journal of Geophysical Research*, vol. 97, p. 4923-4940.

Marone, C., Vidale, J.E. & Ellsworth, W.L. 1995, "Fault healing inferred from time dependent variations in source properties of repeating earthquakes", *Geophysical Research Letters*, vol. 22, p. 3095-3098.
Marone, C. 1998, "The effect of loading rate on static friction and the rate of fault healing during the earthquake cycle", *Nature*, vol. 391, p. 69-72.
Rice, J.R. 1993, "Spatio-temporal complexity of slip on a fault", *Journal of Geophysical Research*, vol. 98, p. 9885-9907.
Richardson, E. & Marone, C. 1999, "Effects of normal stress vibrations on frictional healing", *Journal of Geophysical Research*, vol. 104, p. 28859-28878.
Ruina, A. 1983, "Slip instability and state variable friction laws", *Journal of Geophysical Research*, vol. 88, p 10,359–10,370.
Scholz, C.H. 1998, "Earthquakes and friction laws", *Nature*, vol. 391, p. 37-42.
Scholz, C.H. 2002, *The mechanics of earthquakes and faulting*, Cambridge University Press.
Tullis, T.E. & Weeks, J.D. 1986, "Constitutive behavior and stability of frictional sliding of granite", *Pure and Applied Geophysics*, vol. 124, p. 383-414.
Tullis, T.E. 1996, "Rock friction and its implications for earthquake prediction examined via models of Parkfield earthquakes", *Proceedings of the National Academy of Sciences*, vol. 93, p. 3803-3810.
Ziv, A. & Cochard, A. 2006, "Quasi-dynamic modeling of seismicity on fault with depth variable rate- and state-dependent friction", *Journal of Geophysical Research*, vol. 111, doi:10.1029/2005JB004189.